Supplementary Materials for
Observation of tunable topological polaritons in a cavity waveguide

Dong Zhao,[1,*] Ziyao Wang,[1,*] Linyun Yang,[1] Yuxin Zhong,[1] Xiang Xi,[1] Zhenxiao Zhu,[1] Maohua Gong,[1] Qingan Tu,[1] Yan Meng,[1,†] Bei Yan,[1,‡] Ce Shang,[2,§] and Zhen Gao[1,3,4,¶]

[1]*Department of Electronic and Electrical Engineering, Southern University of Science and Technology, Shenzhen 518055, China.*
[2]*King Abdullah University of Science and Technology (KAUST), Physical Science and Engineering Division (PSE), Thuwal 23955-6900, Saudi Arabia.*
[3]*Laboratory of Optical Fiber and Cable Manufacture Technology, Southern University of Science and Technology, Shenzhen, Guangdong, China.*
[4]*Guangdong Key Laboratory of Integrated Optoelectronics Intellisense, Southern University of Science and Technology, Shenzhen, 518055, China.*

(Dated: March 5, 2024)

CONTENTS

This document includes:
Supplementary Sections S1 to S3
Supplementary Figures S1 to S2

* These authors contributed equally
† mengy@sustech.edu.cn
‡ yanb3@sustech.edu.cn
§ shang.ce@kaust.edu.sa
¶ gaoz@sustech.edu.cn

I. THEORETICAL MODEL

The main text introduces a comprehensive model that captures a dipolar chain embedded in a cavity. This model elucidates the intriguing phenomenon of polariton formation, as represented by Eq. (2) in the main text. Here, we provide a detailed account of the model, which characterizes a general configuration of dipoles. In this setup, each oscillating dp is defined by three fundamental parameters: the effective mass M, the effective charge q of the dipole moment, and the resonance frequency ω_0. We consider these dps as a dimerized chain that is embedded within a cavity waveguide, as illustrated in Fig. S1. The Coulomb interactions among these dipoles give rise to the emergence of collective dipolar excitations, and these excitations, in turn, engage in interactions with the photonic modes in the cavity and lead to the formation of polaritons. We formulate the model of polaritons as the Hamiltonian

$$H_{\mathrm{pol}} = H_{\mathrm{dp}} + H_{\mathrm{ph}} + H_{\mathrm{dp-ph}}, \tag{S1}$$

where H_{dp} is the dipolar Hamiltonian (Sec. I A), H_{ph} is the photonic Hamiltonian (Sec. I B), and $H_{\mathrm{dp-ph}}$ is the light-matter coupling Hamiltonian (Sec. I C).

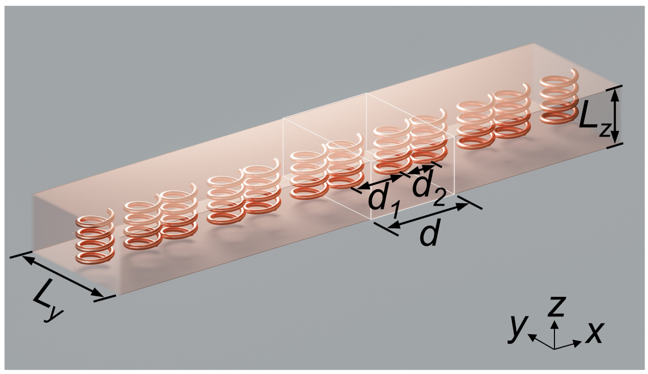

FIG. S1. Sketch of the system. The chain consists of N dimers of dipoles, where the unit cell has two dipoles labeled A and B associated with the resonance frequency ω_0 and the length scale a. The dimerized chain exhibits a period d, defined as the sum of d_1 and d_2.

A. The dipolar Hamiltonian

The dipolar Hamiltonian in Eq. (S1) is given by

$$H_{\mathrm{dp}} = H^{0}_{\mathrm{dp}} + H^{\mathrm{int}}_{\mathrm{dp}}, \tag{S2}$$

where the noninteracting part ($\hbar = 1$ throughout the paper) reads as

$$H^{0}_{\mathrm{dp}} = \sum_{n=1}^{N} \omega_0 \left(a_n^\dagger a_n + b_n^\dagger b_n\right), \tag{S3}$$

corresponding to the Hamiltonian for uncoupled harmonic excitations with resonance frequency ω_0. The index $n \in [1, N]$ denotes the number of dimers in the chain. In Eq. (S3), the bosonic operators a_n $\left(a_n^\dagger\right)$ and b_n $\left(b_n^\dagger\right)$ annihilate (create) an excitation with transverse polarization (oscillating in the z direction) in n-th dimer, where the dipole belongs to the A and B sublattices, respectively. This scheme is depicted in Fig. S1. The long-range dipolar interaction between the excitations is governed by the term $H^{\mathrm{int}}_{\mathrm{dp}}$, which can be split into the intrasublattice Hamiltonian denotes the coupling between the same sublattices (A, A and B, B) and the intresublattice Hamiltonian denotes the coupling between the two inequivalent sublattices (A, B and B, A):

$$H^{\mathrm{int}}_{\mathrm{dp}} = H^{\mathrm{A,A\&B,B}}_{\mathrm{dp}} + H^{\mathrm{A,B\&B,A}}_{\mathrm{dp}}. \tag{S4}$$

The intrasublattice Hamiltonian reads as

$$H^{\mathrm{A,A\&B,B}}_{\mathrm{dp}} = \sum_{n=1}^{N} \sum_{m=n+1}^{N} \frac{\Omega}{(m-n)^3} \left[\left(a_n^\dagger + a_n\right)\left(a_m^\dagger + a_m\right) + \left(b_n^\dagger + b_n\right)\left(b_m^\dagger + b_m\right)\right], \tag{S5}$$

and the intresublattice Hamiltonian reads as

$$H_{\rm dp}^{\rm A,B\&B,A} = \sum_{n=1}^{N} \left[\sum_{m=n}^{N} \frac{\Omega}{\left(m-n+d_1/d\right)^3} \left(a_n^\dagger + a_n\right)\left(b_m^\dagger + b_m\right) + \sum_{m=n+1}^{N} \frac{\Omega}{\left(m-n-1+d_2/d\right)^3} \left(b_n^\dagger + b_n\right)\left(a_m^\dagger + a_m\right) \right]. \tag{S6}$$

Here we introduce the coupling constant $\Omega = \frac{k_x{}^2}{2M\omega_0 d^3} \ll \omega_0$ with the lattice constant $d = d_1 + d_2$, and where d_1 and d_2 are the two central sites separations, as shown in Fig. S1.

Employing the Fourier transforms $a_n = \frac{1}{\sqrt{N}} \sum_{k_x} \mathrm{e}^{ink_x d} a_{k_x}$ and $b_n = \frac{1}{\sqrt{N}} \sum_{k_x} \mathrm{e}^{ink_x d} b_{k_x}$ with the wavevector $k_x = 2\pi p/Nd$ and the integer $p \in [-N/2, +N/2]$ (N should be even), the Eq. (S2) becomes

$$\begin{aligned} H_{\rm dp} = \sum_{k_x} \Big\{ &\left(\omega_0 + \Omega f_{k_x}\right)\left(a_{k_x}^\dagger a_{k_x} + b_{k_x}^\dagger b_{k_x}\right) + \frac{\Omega}{2} f_{k_x}\left(a_{k_x}^\dagger a_{-k_x}^\dagger + a_{-k_x} a_{k_x} + b_{k_x}^\dagger b_{-k_x}^\dagger + b_{-k_x} b_{k_x}\right) \\ &+ \Omega\left[g_{k_x} a_{k_x}^\dagger \left(b_{k_x} + b_{-k_x}^\dagger\right) + g_{k_x}^* \left(b_{k_x}^\dagger + b_{-k_x}\right) a_{k_x}\right] \Big\}, \end{aligned} \tag{S7}$$

with

$$f_{k_x} = 2\sum_{n=1}^{\infty} \frac{\cos(nk_x d)}{n^3} \quad \text{and} \quad g_{k_x} = \sum_{n=0}^{\infty} \left[\frac{\mathrm{e}^{ink_x d}}{\left(n+d_1/d\right)^3} + \frac{\mathrm{e}^{-\mathrm{i}(n+1)k_x d}}{\left(n+d_2/d\right)^3} \right]. \tag{S8}$$

The Hamiltonian (S7) concludes the dipolar excitations in a dimerized chain with long-range interactions. In the nearest-neighbor coupling approximation, the intrasublattice Hamiltonian (S5) is completely neglected, while the intersublattice Hamiltonian (S6) is restricted to $m = n$ and $m = n + 1$, respectively. Therefore, one can get

$$f_{k_x} = 0 \quad \text{and} \quad g_{k_x} = \frac{1}{\left(d_1/d\right)^3} + \frac{\mathrm{e}^{-\mathrm{i}k_x d}}{\left(d_2/d\right)^3}. \tag{S9}$$

B. The photonic Hamiltonian

In Eq. (S1), the photonic Hamiltonian reads as

$$H_{\rm ph} = \sum_{\mathbf{q},\boldsymbol{\lambda}_\mathbf{q}} \omega_\mathbf{q}^{\rm ph} c_{\mathbf{q},\boldsymbol{\lambda}_\mathbf{q}}^\dagger c_{\mathbf{q},\boldsymbol{\lambda}_\mathbf{q}}, \tag{S10}$$

where $c_{\mathbf{q},\boldsymbol{\lambda}_\mathbf{q}}$ $\left(c_{\mathbf{q},\boldsymbol{\lambda}_\mathbf{q}}^\dagger\right)$ annihilates (creates) a photon with wavevector $\mathbf{q}$ and two possible transverse polarizations labeled as $\boldsymbol{\lambda}_\mathbf{q} = \{\mathbf{1}_\mathbf{q}, \mathbf{2}_\mathbf{q}\}$. The photonic mode frequency is $\omega_\mathbf{q}^{\rm ph} = c|\mathbf{q}|$, where c is the speed of light in vacuum and the associated vector potential

$$\mathbf{A}(\mathbf{r}) = \sum_{\mathbf{q},\boldsymbol{\lambda}_\mathbf{q}} \sqrt{\frac{2\pi c^2}{\omega_\mathbf{q}^{\rm ph}}} \left(\mathbf{f}_{\mathbf{q},\boldsymbol{\lambda}_\mathbf{q}}(\mathbf{r}) c_{\mathbf{q},\boldsymbol{\lambda}_\mathbf{q}} + \mathbf{f}_{\mathbf{q},\boldsymbol{\lambda}_\mathbf{q}}^*(\mathbf{r}) c_{\mathbf{q},\boldsymbol{\lambda}_\mathbf{q}}^\dagger\right), \tag{S11}$$

where $\mathbf{f}_{\mathbf{q},\boldsymbol{\lambda}_\mathbf{q}}(\mathbf{r})$ are the mode functions of the photonic cavity [1]. In a cuboid cavity of dimensions $L_x \times L_y \times L_z$, see Fig. S1, the photon wavevector in spherical coordinates read as

$$\mathbf{q} = \begin{pmatrix} q_x \\ q_y \\ q_z \end{pmatrix} = \begin{pmatrix} q_x \\ \frac{\pi n_y}{L_y} \\ \frac{\pi n_z}{L_z} \end{pmatrix} = q \begin{pmatrix} \sin\theta_\mathbf{q} \cos\phi_\mathbf{q} \\ \sin\theta_\mathbf{q} \sin\phi_\mathbf{q} \\ \cos\theta_\mathbf{q} \end{pmatrix}, \tag{S12}$$

where the component q_x is continuous since we take the length L_x of the cavity to be tending towards infinity, n_y and n_z are non-negative integers, arising from hard-wall boundary conditions of the cavity. The spatial profiles of the mode functions then read as [2, 3]

$$\mathbf{f}_{\mathbf{q},\boldsymbol{\lambda}_\mathbf{q}}(\mathbf{r}) = \sqrt{\frac{2}{V}} \begin{pmatrix} \sin\left(q_y y\right) \sin\left(q_z z\right) & \left(\boldsymbol{\lambda}_\mathbf{q} \cdot \mathbf{x}\right) \\ \cos\left(q_y y\right) \sin\left(q_z z\right) & \left(\boldsymbol{\lambda}_\mathbf{q} \cdot \mathbf{y}\right) \\ \sin\left(q_y y\right) \cos\left(q_z z\right) & \left(\boldsymbol{\lambda}_\mathbf{q} \cdot \mathbf{z}\right) \end{pmatrix} \mathrm{e}^{\mathrm{i}q_x x}, \tag{S13}$$

with the cavity volume $V = L_x L_y L_z$. The two-photon polarizations $\boldsymbol{\lambda}_{\mathbf{q}} = \{\mathbf{1}_{\mathbf{q}}, \mathbf{2}_{\mathbf{q}}\}$ are given by

$$\mathbf{1}_{\mathbf{q}} = \begin{pmatrix} \cos\theta_{\mathbf{q}}\cos\phi_{\mathbf{q}} \\ \cos\theta_{\mathbf{q}}\sin\phi_{\mathbf{q}} \\ -\sin\theta_{\mathbf{q}} \end{pmatrix} \quad \text{and} \quad \mathbf{2}_{\mathbf{q}} = \begin{pmatrix} -\sin\phi_{\mathbf{q}} \\ \cos\phi_{\mathbf{q}} \\ 0 \end{pmatrix}. \tag{S14}$$

The photonic mode frequency in Eq. (S10) reads as

$$\omega^{\mathrm{ph}}_{\mathbf{q}} = \omega^{\mathrm{ph}}_{q_x,n_y,n_z} = c\sqrt{q_x^2 + \left(\frac{\pi n_y}{L_y}\right)^2 + \left(\frac{\pi n_z}{L_z}\right)^2}. \tag{S15}$$

In our model, we have $L_x \gg L_y \gg L_z$, and the mode function $\mathbf{f}_{\mathbf{q}\mathbf{2}_{\mathbf{q}}}(\mathbf{r})$ in Eq. (S13) can be simplified as

$$\mathbf{f}_{q_x,n_y}(\mathbf{r}) = \sqrt{\frac{2}{V}} \begin{pmatrix} 0 \\ 0 \\ \sin\left(\frac{\pi n_y y}{L_y}\right) \end{pmatrix} \mathrm{e}^{\mathrm{i}q_x x}. \tag{S16}$$

C. The light-matter interaction Hamiltonian

The light-matter interaction Hamiltonian in Eq. (S1) involves a paramagnetic term $H_{\Pi\cdot\mathbf{A}}$ and a diamagnetic term $H_{\mathbf{A}^2}$, such that [4]

$$H_{\mathrm{dp-ph}} = H_{\mathbf{\Pi}\cdot\mathbf{A}} + H_{\mathbf{A}^2}. \tag{S17}$$

In the long-wavelength approximation $|\mathbf{q}|a \ll 1$, we have explicitly

$$H_{\mathbf{\Pi}\cdot\mathbf{A}} = \sum_{n=1}^{N}\sum_{s=A,B}\frac{Q}{Mc_0}\mathbf{\Pi}_{n,s}\cdot\mathbf{A}\left(\mathbf{r}_{n,s}\right) \tag{S18}$$

and

$$H_{\mathbf{A}^2} = \sum_{n=1}^{N}\sum_{s=A,B}\frac{Q^2}{2Mc_0^2}\mathbf{A}^2\left(\mathbf{r}_{n,s}\right). \tag{S19}$$

The dipole momenta on the A and B sublattices in the dimer n are

$$\mathbf{\Pi}_{n,A} = \mathrm{i}\sqrt{\frac{M\omega_0}{2}}\left(a_n^\dagger - a_n\right)\mathbf{z} \quad \text{and} \quad \mathbf{\Pi}_{n,B} = \mathrm{i}\sqrt{\frac{M\omega_0}{2}}\left(b_n^\dagger - b_n\right)\mathbf{z}, \tag{S20}$$

and the positions of the dips are denoted as

$$\mathbf{r}_{n,A} = \begin{pmatrix} nd - \frac{d_1}{2} \\ \frac{L_y}{2} \\ \frac{L_z}{2} \end{pmatrix} \quad \text{and} \quad \mathbf{r}_{n,B} = \begin{pmatrix} nd + \frac{d_1}{2} \\ \frac{L_y}{2} \\ \frac{L_z}{2} \end{pmatrix}, \tag{S21}$$

In the single photonic band regime, the vector potential of Eq. (S11) becomes

$$\mathbf{A}(x) = \sum_{q_x}\sqrt{\frac{4\pi c^2}{V\omega^{\mathrm{ph}}_{q_x}}}\left(c_{q_x}\mathrm{e}^{\mathrm{i}q_x x} + c^\dagger_{q_x}\mathrm{e}^{-\mathrm{i}q_x x}\right)\mathbf{z}. \tag{S22}$$

By substituting the momenta (S20) and the vector potential (S22), the paramagnetic Hamiltonian (S18) at the positions (S21) reads as

$$H_{\mathbf{\Pi}\cdot\mathbf{A}} = \sum_{k_x}\mathrm{i}\xi_{k_x}\left[\left(a^\dagger_{k_x}\mathrm{e}^{-\mathrm{i}k_x d_1/2} + b^\dagger_{k_x}\mathrm{e}^{\mathrm{i}k_x d_1/2}\right)\left(c_{k_x} + c^\dagger_{-k_x}\right) - \left(c^\dagger_{k_x} + c_{-k_x}\right)\left(a_{k_x}\mathrm{e}^{\mathrm{i}k_x d_1/2} + b_{k_x}\mathrm{e}^{-\mathrm{i}k_x d_1/2}\right)\right], \tag{S23}$$

and the diamagnetic Hamiltonian (S19) reads as

$$H_{\mathbf{A}^2} = \sum_{k_x} \frac{2\xi_{k_x}^2}{\omega_0} \left[c_{k_x}^\dagger \left(c_{k_x} + c_{-k_x}^\dagger \right) + \left(c_{k_x}^\dagger + c_{-k_x} \right) c_{k_x} \right] \tag{S24}$$

with the light-matter coupling constant

$$\xi_{k_x} = \omega_0 \left(\frac{2\pi a^3}{L_y L_z d} \frac{\omega_0}{\omega_{k_x}^{\mathrm{ph}}} \right)^{1/2}, \tag{S25}$$

where $a = \left(\frac{Q^2}{M\omega_0^2}\right)^{1/3}$ is the reparameterized length scale and $\omega_{k_x}^{\mathrm{ph}} = c\sqrt{{k_x}^2 + \left(\frac{\pi}{L_y}\right)^2}$ is the cavity photon frequency.

D. The polaritonic Hamiltonian

With total photonic operators being considered, the polaritonic Hamiltonian can be written as

$$H_{\mathrm{pol}} = \sum_{k_x} \boldsymbol{\psi}_{k_x}^{\mathrm{pol},\dagger} \mathcal{H}_{k_x}^{\mathrm{pol}} \boldsymbol{\psi}_{k_x}^{\mathrm{pol}} \tag{S26}$$

in the basis $\boldsymbol{\psi}_{k_x}^{\mathrm{pol}} = \left(a_{k_x}, b_{k_x}, c_{k_x}^{(0)}, c_{k_x}^{(1)}, c_{k_x}^{(-1)}, \cdots \right)$ and the polaritonic Bloch Hamiltonian reads as

$$\mathcal{H}_{k_x}^{\mathrm{pol}} = \begin{pmatrix} \omega_0 & \Omega g_{k_x} & \mathrm{i}\xi_{k_x}^{(0)} \mathrm{e}^{-\mathrm{i}\chi_{k_x}^{(0)}} & \mathrm{i}\xi_{k_x}^{(1)} \mathrm{e}^{-\mathrm{i}\chi_{k_x}^{(1)}} & \mathrm{i}\xi_{k_x}^{(-1)} \mathrm{e}^{-\mathrm{i}\chi_{k_x}^{(-1)}} & \cdots \\ \Omega g_{k_x}^* & \omega_0 & \mathrm{i}\xi_{k_x}^{(0)} \mathrm{e}^{\mathrm{i}\chi_{k_x}^{(0)}} & \mathrm{i}\xi_{k_x}^{(1)} \mathrm{e}^{\mathrm{i}\chi_{k_x}^{(1)}} & \mathrm{i}\xi_{k_x}^{(-1)} \mathrm{e}^{\mathrm{i}\chi_{k_x}^{(-1)}} & \cdots \\ -\mathrm{i}\xi_{k_x}^{(0)} \mathrm{e}^{\mathrm{i}\chi_{k_x}^{(0)}} & -\mathrm{i}\xi_{k_x}^{(0)} \mathrm{e}^{-\mathrm{i}\chi_{k_x}^{(0)}} & \omega_{k_x}^{\mathrm{ph}(0)} & 0 & 0 & \cdots \\ -\mathrm{i}\xi_{k_x}^{(1)} \mathrm{e}^{\mathrm{i}\chi_{k_x}^{(1)}} & -\mathrm{i}\xi_{k_x}^{(1)} \mathrm{e}^{-\mathrm{i}\chi_{k_x}^{(1)}} & 0 & \omega_{k_x}^{\mathrm{ph}(1)} & 0 & \\ -\mathrm{i}\xi_{k_x}^{(-1)} \mathrm{e}^{\mathrm{i}\chi_{k_x}^{(-1)}} & -\mathrm{i}\xi_{k_x}^{(-1)} \mathrm{e}^{-\mathrm{i}\chi_{k_x}^{(-1)}} & 0 & 0 & \omega_{k_x}^{\mathrm{ph}(-1)} & \\ \vdots & \vdots & \vdots & & & \ddots \end{pmatrix} \tag{S27}$$

with the general photon dispersion

$$\omega_{k_x}^{\mathrm{ph}(m)} = c\sqrt{\left(k_x - \frac{2\pi m}{d}\right)^2 + \left(\frac{\pi}{L_y}\right)^2}, \quad m = 0, \pm 1, \pm 2, \ldots, \tag{S28}$$

the light-matter coupling constant

$$\xi_{k_x}^{(m)} = \omega_0 \left(\frac{2\pi a^3}{L_x L_y d} \frac{\omega_0}{\omega_{k_x}^{\mathrm{ph}(m)}} \right)^{1/2}, \tag{S29}$$

and χ_{k_x}

$$\chi_{k_x}^{(m)} = \frac{d_1}{d} \left(\frac{k_x d}{2} - m\pi \right). \tag{S30}$$

The quantities in the winding vector read

$$\omega_{0,j} = \omega_0 + \sum_{m=-\infty}^{+\infty} \frac{{\xi_{k_x}^{(m)}}^2}{\omega_{k_x,j}^{\mathrm{pol}} - \omega_{k_x}^{\mathrm{ph}(m)}}, \quad h_{k_x,j} = g_{k_x} + \frac{1}{\Omega} \sum_{m=-\infty}^{+\infty} \frac{\mathrm{e}^{-2\mathrm{i}\chi_{k_x}^{(m)}} {\xi_{k_x}^{(m)}}^2}{\omega_{k_x,j}^{\mathrm{pol}} - \omega_{k_x}^{\mathrm{ph}(m)}} \tag{S31}$$

with the polariton eigenfrequencies $\omega_{k_x,j}^{\mathrm{pol}}$.

II. PHASE TRANSITIONS

In this section, we analyze the phase transition of the models in the rotating-wave approximation (RWA). The RWA is appropriate when the frequencies of all modes are close to resonance.

A. SU(3) polaritonic model

After disregarding the counter-rotating terms which correspond to the approximation for $\Omega \ll \omega_0$, the polaritonic Hamiltonian denotes as

$$\begin{aligned} H_{\text{pol}}^{\text{RWA}} = \sum_{k_x} \Big[& \omega_0 \left(a_{k_x}^\dagger a_{k_x} + b_{k_x}^\dagger b_{k_x} \right) + \Omega \left(g_{k_x} a_{k_x}^\dagger b_{k_x} + g_{k_x}^* b_{k_x}^\dagger a_{k_x} \right) + \omega_{k_x}^{\text{ph}} c_{k_x}^\dagger c_{k_x} \\ & + \mathrm{i}\xi_{k_x} \left(a_{k_x}^\dagger \mathrm{e}^{-\mathrm{i}k_x d_1/2} + b_{k_x}^\dagger \mathrm{e}^{\mathrm{i}k_x d_1/2} \right) c_{k_x} - \mathrm{i}\xi_{k_x} c_{k_x}^\dagger \left(a_{k_x} \mathrm{e}^{\mathrm{i}k_x d_1/2} + b_{k_x} \mathrm{e}^{-\mathrm{i}k_x d_1/2} \right) \Big], \end{aligned} \tag{S32}$$

and can be alternatively written as

$$H_{\text{pol}}^{\text{RWA}} = \sum_{k_x} \boldsymbol{\psi}_{k_x}^{\text{pol},\dagger} \mathcal{H}_{k_x}^{\text{pol,RWA}} \boldsymbol{\psi}_{k_x}^{\text{pol}} \tag{S33}$$

in the basis $\boldsymbol{\psi}_{k_x}^{\text{pol}} = (a_{k_x}, b_{k_x}, c_{k_x})$ with the polaritonic Bloch Hamiltonian

$$\mathcal{H}_{k_x}^{\text{pol,RWA}} = \begin{pmatrix} \omega_0 & \Omega g_{k_x} & \mathrm{i}\xi_{k_x}\mathrm{e}^{-\mathrm{i}\chi_{k_x}} \\ \Omega g_{k_x}^* & \omega_0 & \mathrm{i}\xi_{k_x}\mathrm{e}^{\mathrm{i}\chi_{k_x}} \\ -\mathrm{i}\xi_{k_x}\mathrm{e}^{\mathrm{i}\chi_{k_x}} & -\mathrm{i}\xi_{k_x}\mathrm{e}^{-\mathrm{i}\chi_{k_x}} & \omega_{k_x}^{\text{ph}} \end{pmatrix}. \tag{S34}$$

equation (S34) corresponds to Eq. (2) in the main text (which is $\mathcal{H}_{\text{pol}}$ as dropping the k_x subscripts for simplicity) and forms the SU(3)[43, 44] group. The polaritonic Zak phase gives

$$\theta_{\text{pol}}^{\text{Zak}} = \mathrm{i} \int_{-\pi/d}^{+\pi/d} dk_x \left\langle \psi_{k_x,j}^{\text{pol}} \left| \partial_{k_x} \right| \psi_{k_x,j}^{\text{pol}} \right\rangle, \tag{S35}$$

with the polariton band index $j = \{1, 2, 3\}$.

B. SU(2) polaritonic model

In Sec. II A, we have shown how the polaritonic Bloch Hamiltonian (S34) can be written as a 3×3 matrix in the SU(3) group. By eliminating the photonic degree of freedom, we rewrite the Hamiltonian (S34) as an effective 2×2 matrix Hamiltonian in the SU(2) group:

$$\mathcal{H}_{k_x,j}^{\text{pol,RWA}} = \begin{pmatrix} \omega_{0,j} & \Omega h_{k_x,j} \\ \Omega h_{k_x,j}^* & \omega_{0,j} \end{pmatrix} = \omega_{0,j}\mathcal{I}_0 + \boldsymbol{\sigma} \cdot \boldsymbol{w}_{k_x,j}, \tag{S36}$$

and where the renormalized on-diagonal frequency $\omega_{0,j}$ and off-diagonal quantity $h_{k_x,j}$ are defined via

$$\omega_{0,j} = \omega_0 + \frac{\xi_{k_x}^2}{\omega_{k_x,j}^{\text{pol}} - \omega_{k_x}^{\text{ph}}}, \quad h_{k_x,j} = g_{k_x} + \frac{\mathrm{e}^{-2\mathrm{i}\chi_{k_x}}}{\Omega} \frac{\xi_{k_x}^2}{\omega_{k_x,j}^{\text{pol}} - \omega_{k_x}^{\text{ph}}} \tag{S37}$$

with the three polaritonic eigenfrequencies $\omega_{k_x,j}^{\text{pol}}$ [by taking the dominant $m = 0$ in Eq. (S30)]. Now we have an effective winding vector $\boldsymbol{w}_{k_x,j}$, with the components

$$w_{k_x,jx} = \Omega \left| h_{k_x,j} \right| \cos\varphi_{k_x,j}, \quad w_{k_x,jy} = -\Omega \left| h_{k_x,j} \right| \sin\varphi_{k_x,j}, \quad \mathrm{e}^{\mathrm{i}\varphi_{k_x,j}} = \frac{h_{k_x,j}}{\left| h_{k_x,j} \right|}. \tag{S38}$$

begindocument

III. EDGE STATES

Figure S2(a) shows the simulated [white (cyan) dots represent the bulk (edge) states] and measured (color maps) polaritonic eigenfrequencies as a function of L_y. The topological edge states in the bandgap are localized at the right end of the MRHs chain, as shown in Fig. S2(b).

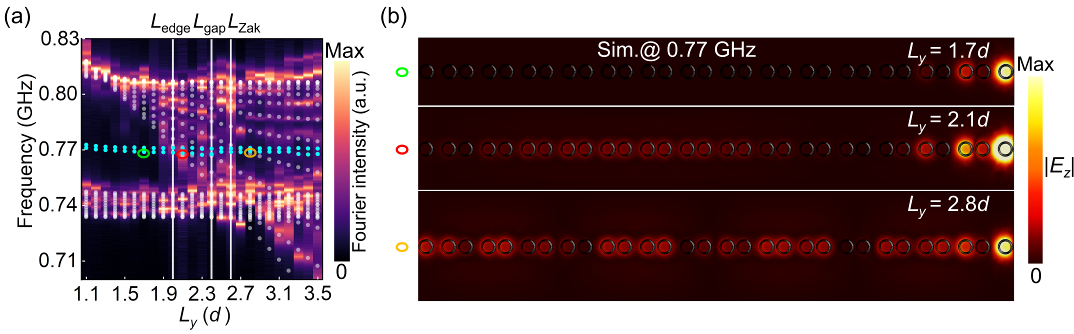

FIG. S2. Tunable topological phases of polaritons by changing the cavity waveguide width L_y. (a) Measured (color map) and simulated (white dots) eigenfrequency diagram of a 1D finite dimerized chain of 30 MHRs embedded in a cavity waveguide as a function of L_y. The simulated topological edge states are represented by cyan dots. (b) Simulated electric field distributions of the topological edge states at 0.77 GHz with $L_y = 1.7d$ (green ellipse), $2.1d$ (red ellipse), and $2.8d$ (brown ellipse), respectively.

[1] P. W. Milonni, *The quantum vacuum: an introduction to quantum electrodynamics* (Academic press, 2013).

[2] K. Kakazu and Y. S. Kim, Quantization of electromagnetic fields in cavities and spontaneous emission, Phys. Rev. A **50**, 1830 (1994).

[3] T. J. Sturges, T. Repän, C. A. Downing, C. Rockstuhl, and M. Stobińska, Extreme renormalisations of dimer eigenmodes by strong light-matter coupling, New J. Phys. **22**, 103001 (2020).

[4] C.-R. Mann, T. J. Sturges, G. Weick, W. L. Barnes, and E. Mariani, Manipulating type-I and type-II Dirac polaritons in cavity-embedded honeycomb metasurfaces, Nat. Commun. **9**, 2194 (2018).